CubeSat System to Image Ceres

EECS 430: Wireless Link Design

Group 3 Final Design Report

By: Jack Gregory, Raheida Khalique, Lexie Roberts, Gabe Ronan, Katy Wolff

Project Summary

Launched in 2007, the NASA Dawn mission orbited the dwarf planet Ceres to image and determine the evolution of the planet. Our project focuses on designing a system that will help us image Ceres in further detail. The system consists of a synthetic aperture radar link for imaging Ceres and a data link to communicate the image data with a larger orbiting satellite, which would then downlink the processed data to an Earth-based ground station. For this winter semester, we have focused on designing one component of this overall system.

Objectives

We have three main goals for our system. The first objective was to design the radar link to image Ceres and the data link between the CubeSat and larger satellite. We designed a synthetic aperture radar (SAR) system because it was successfully used in previous NASA missions, including Dawn, for imaging purposes. The second goal was to design the SAR antenna, solar panels, and their deployment processes. The third part of our project was to develop a hypothetical test plan for our system.

Our overall system consists of an Earth-based ground station, CubeSat antenna radar system, and larger orbiting satellite. The larger satellite will function as a communications relay with the Earth-based ground station to then downlink the processed SAR data. It will also be used to launch our CubeSat system off of. Our project is focusing only on the radar and data link of the CubeSat system, the SAR antenna and solar panel design, and deployment mechanisms.

Requirements

For our link analysis, we are using the radar equation $\frac{P_R}{P_N} = \frac{P_t GG\ \sigma\lambda^2}{(4\pi)^3 R^4}\frac{1}{KTB}$ [1]. This equation contains the following terms and also assumes the transmit and receive antennas are identical:

$P_R =$ received power (W)
$P_N =$ noise power (W)
$P_t =$ transmit power (W)
G = gain of transmit, receive antennas (W)
σ = radar cross section (m^2)
λ = wavelength of signal (m)
R = orbiting altitude (m)
K = Boltzmann's constant = $1.38 * 10^{-23}\ \frac{W}{Hz\cdot K}$
T= temperature (K)
B = bandwidth (Hz)

We need to achieve a signal-to-noise ratio (SNR) of 10 to 20 dB to ensure the imaging data is received reliably. This is based on SNR of previous SAR missions. A medium antenna gain (10 to 20 dB) is required to achieve this SNR.

The customer presented the project to our team as an open-ended design problem. We worked with the customer to determine image resolutions and antenna size specifications that would image Ceres with further detail than previous missions. The orbit radius, swath width, and antenna look angle are the parameters that drive the design of the SAR imaging parameters, such as azimuth and range resolution.

The antenna dimensions are constrained to fit within a 6U CubeSat. With the inclusion of deployment mechanisms, this requirement can be achieved.

Range resolution is defined [3] as $R_r = \frac{c}{2B\sin(\theta)}$ where :

c = speed of light (m/s)
B = bandwidth (Hz)
θ= antenna look angle (radians)

Azimuth resolution is defined [3] as $R_a = \frac{L}{2}$ where L is the length of the antenna in the azimuth direction.

Discussing with our customer, the length of the antenna was chosen as double the length of the 6U CubeSat. This corresponds to an antenna length of 1.2 meters. This length yields an azimuthal resolution of 0.6 m according to the formula listed above. A long antenna generates a more concentrated radar beam, which is advantageous because a large swath width and a more concentrated beam produces more data points per signal transmitted. More data points increases our image resolution, and therefore detail of geological structures on Ceres. A more detailed explanation of the radar imaging resolution is included in the *Radar Resolution* section of this report.

The range resolution depends on the look angle and bandwidth of the system according to the formula listed above. Discussing with our customer, we chose to design for a range resolution of 58 m as detailed in the *Radar Resolution* section.

We selected a frequency in the X-band, 10 GHz, for several reasons. First, the Dawn spacecraft that we used as a model for our system used a similar frequency. More importantly, higher radio frequencies are more highly attenuated by rain [4]. We chose 10 GHz as a mid-range frequency in the X-band. It is important to note that this decision was an artificial constraint on our system, and different frequency choices are explored in the *Recommendations for Spaceflight* section.

Several conditions in spaceflight must be considered in the design of the CubeSat system [2]. Radiation from the sun will heat the CubeSat system, but the temperature in space in the satellite's orbit will be extremely cold. These drastic environmental changes require that selected components function in both low and high temperatures. A standard temperature range for radiation-hardened components is -55 °C to 125 °C. Additionally, the sun's high levels of radiation can damage circuit boards. Therefore, the circuit components must be designed and selected to withstand radiation.

Table 1: Requirements Table. This table reflects the parameters chosen after discussing with our customer and are the design drivers of our system.

Range Resolution	58.0 m
Azimuth Resolution	0.6 m
Frequency	7 to 12 GHz (X-band)
Temperature	-55 °C to 125 °C

Background Information

Ceres

Ceres is the largest object and only current dwarf planet contained in the asteroid belt [5] and is about 1/13th the size of Earth. In 2007, the Dawn spacecraft, the first mission to orbit two extraterrestrial destinations and a dwarf planet, was launched. From the four types of data returned by Dawn, scientists concluded two main points. The first is that location is key to how objects formed early on. Location determines the amount of water incorporated into objects in the solar system and water plays an important role in driving out heat. From this discovery, scientists decided bodies like Ceres formed with a lot of water and cooled quickly which resulted in Ceres' outer shell to be composed of water dried in the form of ice and hydrates. Second, the surface of Ceres contains organic molecules including Carbon and those molecules associated with Earth's oceanic and lake environments. Additionally, the magnesium sulfate deposits demonstrate how well the surface of Ceres reflects sunlight.

The Dawn mission mapped the surface of Ceres using a Visual and Infrared Imaging Spectrometer (VIR) to determine its composition, temperature and properties[18]. The VIR instrument "sees" in the visible and infrared ranges. Maps of the elements on the planet's surface illustrated mysterious pyramids and volcanoes on Ceres. Because scientists believe Ceres contains water below its surface and liquids enriched in salt would lower the freezing point, there is reason to believe in recent geological activity. The mission concluded in 2018 because the spacecraft ran out of fuel. Dawn gave scientists reason to believe the dwarf planet could have hosted life or oceans in the past given its surface anatomy.

Synthetic Aperture Radar

To image the surface of Ceres, we decided to design a synthetic aperture radar (SAR) system. SAR systems work by using the motion of the antenna in order to increase the size of the antenna aperture synthetically. This technique allows us to get higher resolution images than we could acquire with a typical stationary radar. SAR systems also use a side-looking beam in order to further increase the resolution in the direction perpendicular to the direction of travel.

Several factors led us to choose SAR to image the surface of Ceres. First, because SAR uses the motion of the antenna in order to create a larger effective aperture size, a smaller antenna is required. The radar motion introduces a Doppler frequency shift that enables the resolution of nearby points. Therefore, we can design an antenna to fit on a 6U CubeSat. Also, SAR systems have been used many times to image planetary surfaces. The DAWN mission and the RainCube CubeSat mission both utilized SAR, which means that we will have a large foundational knowledge base that we can reference when designing our system. For these reasons, we believe that SAR will be the most effective design for imaging the surface of Ceres.

Radar Resolution

The resolution of SAR imaging is defined in two parts, the range resolution and the azimuth resolution. The range resolution is defined in the direction perpendicular to the direction of travel. It depends on the pulse width of the signal that is being transmitted by the radar. Based on the pulse width of the signal and the amount of time that it takes for the signal to be transmitted from the radar, reflected off of the ground, and received back by the radar there are a certain number of unique pixels that occur with no overlap. Typically, there can be multiple independent pixels per swath width. Alternatively, the azimuth resolution is defined in the direction parallel to travel. It is defined as half of the length of the antenna in the azimuth direction [3]. Therefore, it is typically much higher than the resolution of a stationary radar, which is proportional to the slant range and wavelength [3].

Design Ideas

Antenna Design

An antenna with a narrow vertical beam is achieved with a wide vertical dimension [6]. Fan beam antennas are characterized by a narrow vertical beam pattern, making them well-suited for radar applications which require a narrow beam for detailed resolution. We considered various antenna designs, including fan beam and microstrip patch antennas. The viability of each antenna is based on its gain, and ease of design and manufacturing. The goal is to design an antenna with a narrow azimuthal beamwidth in order to resolve detail in nearby objects. Two objects are resolvable within a radar swath if they are not both located in the antenna beamwidth [3]. A narrow beamwidth allows for higher image resolution, helping us achieve the goal of improving the image resolution compared to the Dawn mission.

We considered a microstrip patch antenna design. However, this design would require fine tuning in HFSS to optimize the array and is more difficult to impedance match. Therefore, a fan beam antenna was selected since it is characterized by a narrow azimuthal bandwidth and is straightforward to design and test.

Many options exist for an antenna with a fan beam radiation pattern. Paraboloid reflectors are commonly implemented fan beam antennas. A reflector antenna's gain is proportional to its diameter and inversely proportional to the wavelength [7]. The wavelength of our system is 0.03 m, so the diameter of the reflector antenna could be designed to fit within the 6U cubesat. Modeling and fabrication of a reflector antenna could prove difficult for the short term focus of our project. Ultimately, our customer recommended a slotted waveguide antenna as the choice of fan beam antenna, since it is simple to model and fabricate. We chose to design the slotted waveguide antenna with aluminum, since its conductivity is similar to that of copper yet is a cheaper alternative to copper. Its radiation pattern is that of a fan beam antenna which directs radiation along the swath width on Ceres. It folds in half inside of the 6U CubeSat, allowing for a compact yet simple design to achieve our design specifications.

Hinge Design

Since the 1.2 meter long antenna will not fit directly into the 6U CubeSat, we have chosen a hinge mechanism to unfold the antenna on the outside of the CubeSat after deployment. We selected a GoPro camera hinge as an initial proof-of-concept design. We anticipate possible impedance mismatches or reflections caused by the hinge and analyze these effects in the *Capacitive Coupling* section later in the report.

Figure 1: This image depicts a CAD model of the hinge design for our model.

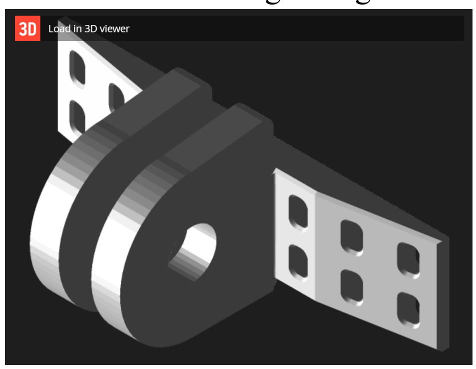

Radar Link Design

There are two types of radar designs we could implement in our overall system. Monostatic radar implements the transmitter and receiver on a single antenna. This is the simpler radar implementation but requires a high power transmission from the single CubeSat. Since the solar panels on the CubeSat cannot supply enough transmit power, bistatic radar will be implemented, but we are only designing one radar link portion. The *Solar Panels* section discusses the transmit power available from the solar panels that will be mounted on the CubeSat. Bistatic radar implements the transmitter and receiver on separate spacecraft and antennas. This radar set-up spreads out the necessary transmit power for the system.

As a prototype design, we have designed a radar wireless link to image Ceres, capturing image information and transmitting the data to a larger spacecraft also orbiting Ceres. The slotted waveguide antenna will transmit and receive data to image Ceres and a separate data link (discussed in the *Data Link Analysis* section) will be used to transmit the captured data to the spacecraft for processing. This design strategy reduces the strain on the solar panels of the CubeSat and spreads the power required in the system to multiple antennas.

Considering all of these limitations, we designed our SAR link to have the following parameters. The bandwidth of 10 MHz is based on bandwidths most commonly used in previous SAR applications, and the swath width had to be small enough to make multiple passes over Ceres, which has a diameter of 940 km[18]. Decreasing the look angle of the antenna also contributed to decreasing the swath width. For a given swath width and look angle, our orbit radius of 130 km is calculated.

Table 2: This table displays the parameters for our SAR system.

Antenna Length	1.2 m
Antenna Width	0.03 m
Look Angle	15 degrees
Orbit Radius	130 km
Bandwidth	10 MHz
Pulse Width	0.1 microseconds
Range Resolution	58.0 m
Azimuth Resolution	0.6 m
Swath Width	139 km

From the parameters above, we plugged in these values into the radar equation $\frac{P_R}{P_N} = \frac{P_t GG\ \sigma\lambda^2}{(4\pi)^3 R^{\ 4}} \frac{1}{KT\ B}$. This makes the assumption that the transmit and receive antennas are identical. Calculations for the transmit power are given in the solar panels section. The radar cross-section value for Ceres was found in several papers analyzing the use of radar to image Ceres[13][14][15][16]. Radar cross-section is defined as the target's ability to reflect radar signals in the direction of the radar receiver, or the measure of the backscatter power per received power density, and is constant for both stationary and SAR applications [21]. Also, the temperature of Ceres is much colder than Earth[18]. Ultimately, our SNR far exceeds the 10 to 20 dB goal.

Table 3: This table displays the parameters for our radar link design.

Transmit Power	0.15 W/per cell
Number of Solar Cells	1
Antenna Gain	23.7 dB
Radar Cross-Section	$2.52*10^{10}$ m^2
Antenna Area	0.036 m^2

Orbit Radius	130 km
T	150 K
Bandwidth	10 MHz
SNR	26.7 dB

In actuality, our transmit power for our system would be much higher as this design is based on the assumptions that the antenna is 100% efficient and is the only component being powered. Our CubeSat would have other subsystems such as command and data handling, and attitude determination and control, that would need to be powered. Including these systems and others and accounting for more losses and inefficiencies would put us closer to the 40 W operating power of the JPL RainCube [22].

The antenna will be placed on the side of the CubeSat facing downwards to Ceres and will be oriented at a 15 degree look angle as previously described. The solar panels will be on the top of the CubeSat facing toward the sun. We will alternate operating our radar and data links while the CubeSat is in view of the sun.

Transmit Power Solar Panels

Our favored products for supplying power to the antenna are the EXA Deployable Solar Panels DSA/1A and the 3U Single Deployable Solar Array from EnduroSAT [8]. These solar cells can supply up to 0.15 watts per cell accounting for the solar constant at Ceres and the cell area and efficiency. With the correct deployment mechanism, we are confident that we can link a sufficient number of these multi-cell panels together to produce the required power.

We used the following equation to calculate the possible transmitted power from the solar cells [17].

Transmit power = # solar cells*solar constant from sun*1/distance to Ceres (Au) squared* solar cell area*solar cell efficiency

$1*1366\ W/m^2*(1/2.8)^2*0.0027\ m^2*0.29 = 0.15$ W per cell

When we accounted for an estimated antenna efficiency of 80%, we found that the SNR decreased by 1 dB, which will not have a significant effect on the quality of the link. Also, reducing the gain of the antenna to 20 dB decreases the SNR to 9.6 dB, so the gain of the antenna has a significant effect. By at least accounting for the solar panel efficiency we have calculated a reasonable estimate of the transmitted power from the solar cell.

Figure 2: (Left) This figure demonstrates the number of cells vs. SNR in dB. As the number of solar cells increases, the SNR increases. (Right) This figure is an image of the EXA deployable solar panels we have chosen.

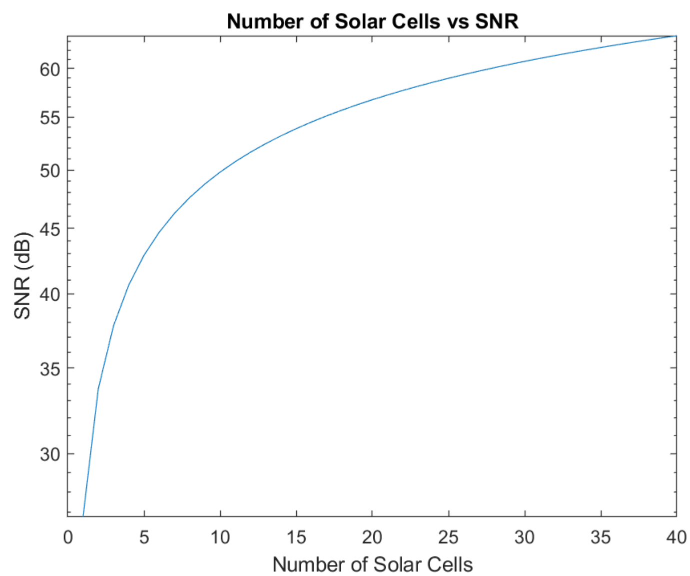

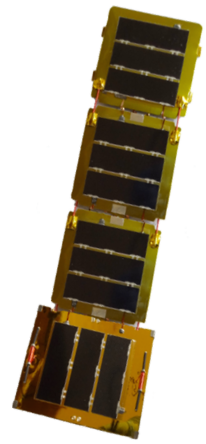

Data Link Design

The design for our satellite dictates raw data collection only. Significant capabilities for data processing are assumed to be available on a nearby satellite where we will eventually transmit the data. Therefore this data link analysis will approximate only the bit error rate for our cubesat system receiving its own gathered data from the surface of Ceres. A full link analysis between our cubesat and a master satellite requires specific parameters for the receiving system and appropriate modulation schemes, which is beyond the scope of this report.

For most raw SAR imaging data, the size of each sample is about 10 bits. We only need to measure the amplitude of the returned pulse. More detailed image analysis can include measurement of the polarization as well, but here we will only be considering signal strength. From our findings we see that the sampling rate is equal to the pulse repetition frequency, which is bounded below and above by functions derived from the definitions of pulse length, swath width, and satellite velocity [11]. These bounds are 524.80 Hz to 538.22 Hz. The worst case sampling rate is 538.22 Hz, and multiplying this by the number of bits per sample gives a maximum bit rate of 5.38 kilobits per second, or 672.5 bytes per second [12]. In order to approximate the received energy per bit to noise density, we can use that fact that our signal bandwidth is well defined. Therefore can approximate the bit signal-to-noise ratio as the antenna SNR (26.7 dB) divided by the “gross” link spectral efficiency in bits/(s*Hz) [24]. Link spectral efficiency is the maximum throughput (5.38 kilobits/s) divided by the bandwidth in hertz (10 MHz). This results in a ratio of received energy per bit to noise density of about 59.4 dB.

Table 4: This table displays the parameters and equations for the data link design.

Altitude	$400e3\ m$
Ceres Radius, rad_c	$473e3\ m$
Orbit Radius	$873e3\ m$
Speed of light, c	$3e8\ m/s$
Frequency, f	$10e9\ Hz$
Angle, θ	$\frac{15\pi}{180}$
Antenna Length, L	$1.2\ m$
Wavelength, λ	$0.03\ m$
Pulse width, τ	$\frac{1}{10e6} = 1 * 10^{-7}\ s$
Antenna Width, W_a	$0.03\ m$
Gravitational Constant, G	$6.67408e - 11\ \frac{m^3}{kg\ s^2}$
Ceres Mass, M_C	$8.958e20\ kg$

$$Orbit\ Radius = altitude + rad_c,\ where\ rad_c = radius\ of\ Ceres$$

The velocity of the spacecraft relative to the ground is given by $Velocity = \sqrt{\frac{G \cdot M_C}{orbit\ radius}}$. The lower bound is obtained using the velocity and is defined as $Lower\ bound = \frac{2 \cdot velocity}{L}$ and gives the minimum pulse repetition frequency. In a repeating signal, the pulse repetition frequency (PRF) is the number of pulses per second. Because the PRF cannot be too large, an upper bound is calculated using $Upper\ bound = \frac{1}{2\tau + 2\frac{2 \cdot Swath}{c}}$. The swath width, $Swath = \frac{\lambda R_{mid}}{W_a cos(\theta)}$, is calculated using the near and end range distances and the angle between broadside to the antenna. The equation $R_{mid} = \frac{altitude}{cos(\theta)}$ is the halfway distance between radar and illumination pattern, separating the look angles to the near and far ranges[12][13].

Antenna Design

We chose to design a slotted waveguide antenna because it is simple to design and manufacture compared to other fan beam antenna choices previously mentioned, like an array of microstrip patch antennas. It has also previously been used in SAR applications. If we were to test our antenna, we would feed it with a coax to WR90 adapter found on Ebay. Our slotted waveguide antenna uses a WR90 waveguide which operates between 8.2 and 12.4 GHz and is 22.86 mm wide and 10.16 mm tall. The wall thickness is designed to be 2.50 mm, and the slots have the following specifications based on antenna theory[23]:

Table 5: This table displays the parameters of our slotted waveguide antenna.

Frequency	10 GHz
# of Slots	30
Slot Length	19.875 mm
Slot Width	1.9875 mm
Slot Offset	0.4246 mm
Antenna Length	1.2 m
Antenna Width	0.03 m

Figure 3: This figure shows a zoomed-out picture of our slotted waveguide antenna in a CAD program.

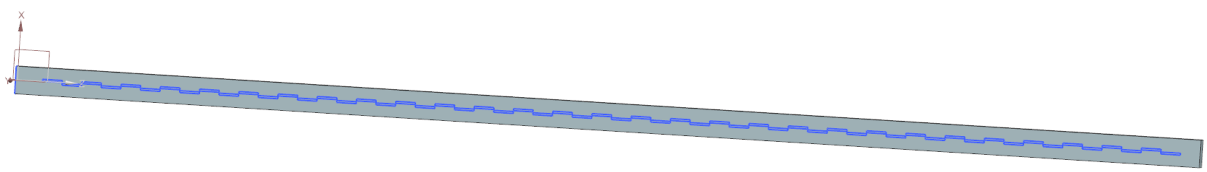

Figure 4: This figure shows a zoomed-in picture of a portion of slots, offset from the center line to increase the impedance of each slot, and are each a half-guided wavelength long and guided wavelength/20 wide. The antenna has 30 slots.

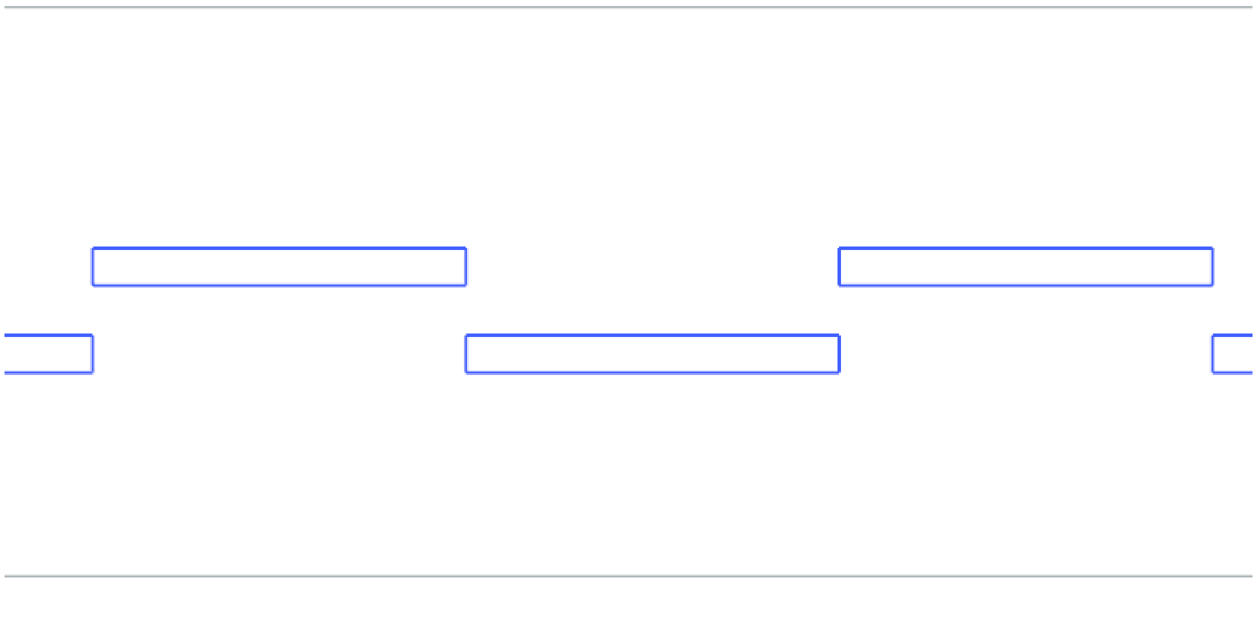

Deployment

Even with the implementation of SAR, we will need to select a deployment mechanism for the antenna as well as the solar panels. There are several antenna deployment strategies that previous missions have used. The antenna could unfold in an upside-down umbrella shape or unfold in panels. A microstrip patch antenna array could be deployed in a sequence of panels, while a dish antenna could be deployed in an umbrella shape.

We plan to deploy our slotted waveguide antenna using a sliding lock mechanism, similar to that of a ski boot. Once the antenna is slid to the outside of the CubeSat, the antenna will unfold from its central hinge and lock in place. The EXA deployable solar panels have a similar unfolding mechanism.

Simulation Results

Antenna Performance

We have simulated the antenna performance using HFSS and have measured its radiation pattern and electric field coupling. We can show that the antenna gain is 23.7 dB and is of a characteristic fan beam pattern. Also, the input impedance is 48.7 ohms and the return loss at 10 GHz is -17 dB**.**

Figure 5: This figure shows the electric field coupling of the individual slots of the slotted waveguide antenna. The field plots show that the slots effectively radiate electromagnetic energy, confirming our design works.

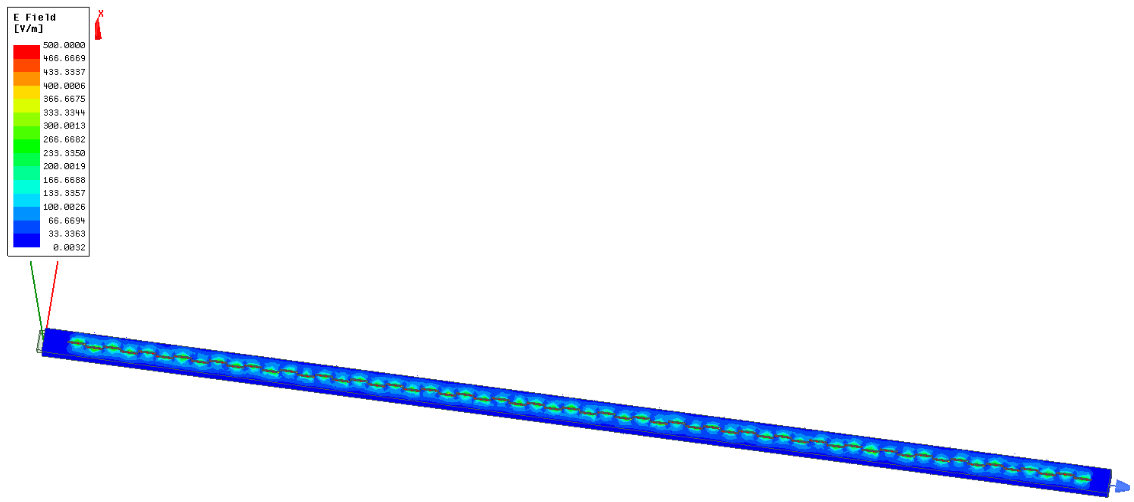

Figure 6: This figure shows the radiation pattern and gain of the slotted waveguide antenna. The high gain, shown in red, is concentrated at the center of the pattern. This is the desired radiation pattern of a fan beam antenna, and the main reason we chose the slotted waveguide design. The radiation pattern will be concentrated on the swath width of the radar and enable imaging data to be received.

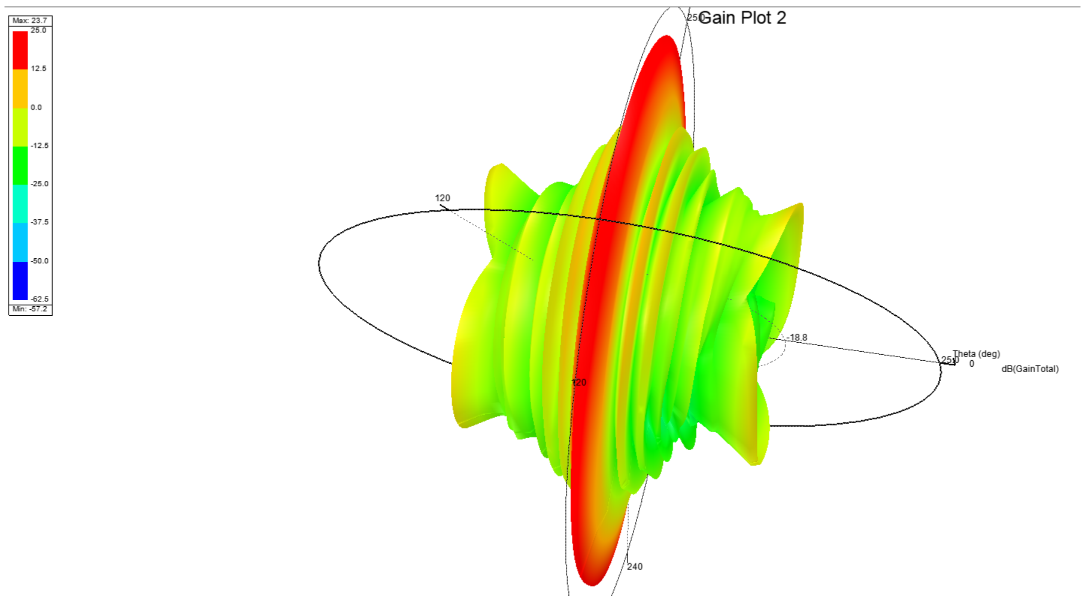

Figure 7: This figure shows the input impedance of the antenna. At 10 GHz, the antenna impedance is 48.7 ohms which means it is a good match to a 50 ohm feed.

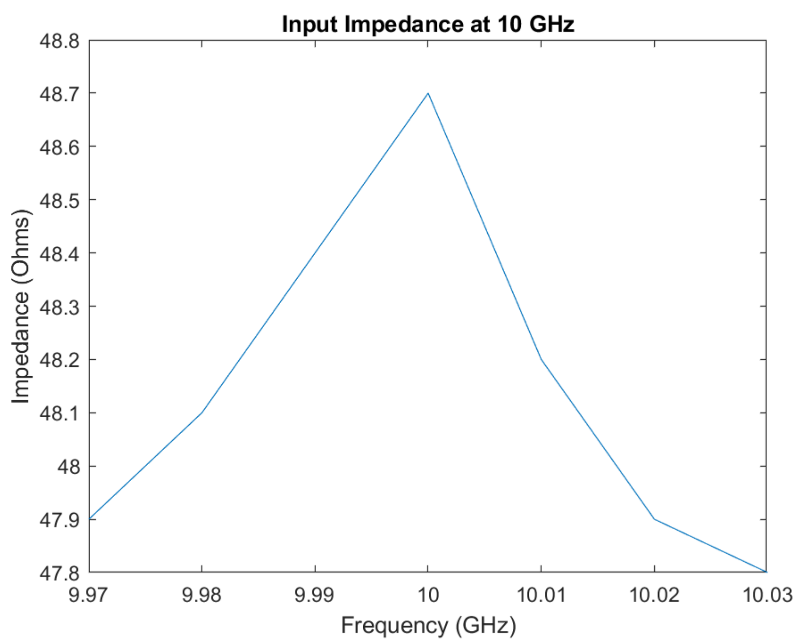

Figure 8: This figure shows the return loss of the antenna, which is a measure of the amount of reflection of the signal, instead of transmitting outward. A more negative return loss means more of the signal is being transmitted from the antenna and not being reflected back. A return loss of -17 dB means the antenna functions with minimal reflections at 10 GHz.

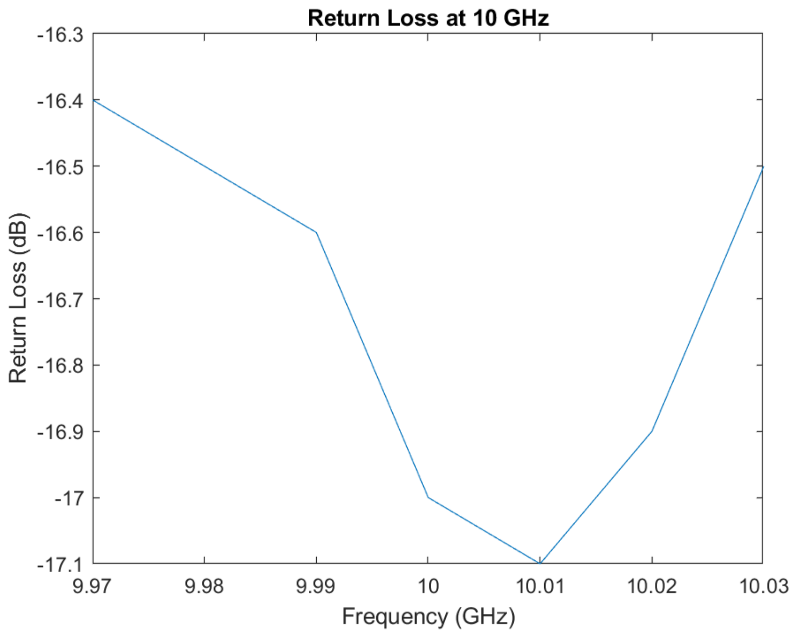

Capacitive Coupling at Hinge

As the metal of the antenna oxidizes, there is concern that this could create a capacitive effect between the two halves of the antenna. To approximate the impedance of this capacitance, we modelled the two waveguide flanges of the halves as a parallel plate capacitor, with area 0.000232 m^2 calculated from the dimensions of the WR90 waveguide. The capacitance of a parallel plate is $C = \varepsilon A/d$ where d is the distance between the waveguide halves. The impedance of a capacitor is then $X = 1/(\omega * C)$ where ω is 2*pi*frequency. The frequency used was 10 GHz. This calculation is plotted below. In conclusion, the capacitive coupling at the hinge of the antenna is very much a non-negligible effect and would increase the antenna input impedance, worsening the match to a 50 ohm feed. This effect needs to be resolved and is discussed in the *Recommendations for Spaceflight* section, and it is very important that the two halves are secured together tightly to minimize this effect.

Figure 9: This figure shows how capacitive impedance increases as the distance between antenna halves is increased.

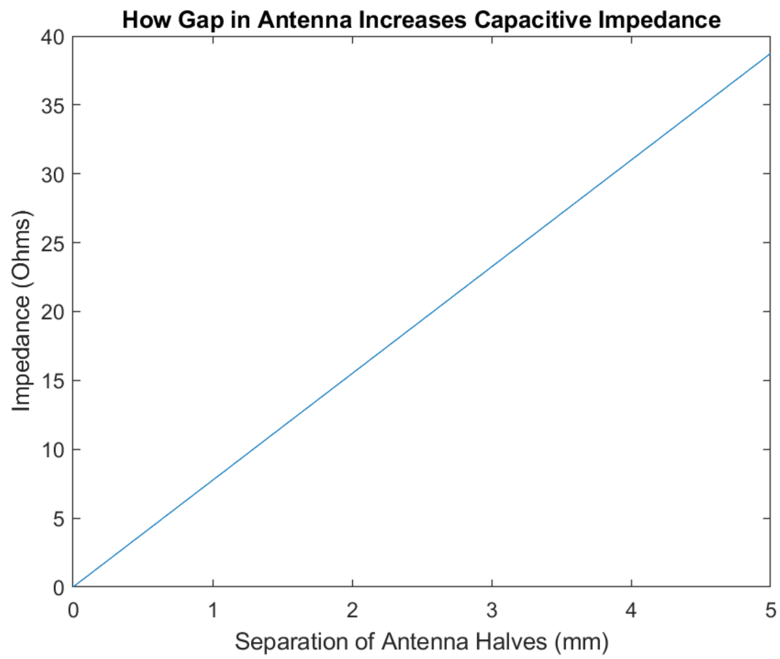

Proposed Test Plan

Our test plan seeks to measure and characterize four parameters to prove that our system concept works properly. First, we will be measuring the antenna input impedance as well as the voltage standing wave ratio (VSWR). With these measurements, we would like to confirm that our antenna is matched, or close to matched, to a 50 ohm transmission line. We would also like to measure the S11 parameter and produce a plot to confirm that the operating frequency of our antenna is close to its operating frequency, 10 GHz. The final test that we would like to perform is a far-field radiation pattern characterization. We will do this both in the horizontal and vertical planes and compare the results with those simulated in HFSS.

Antenna Input Impedance

In order to measure the input impedance of our antenna, we will use a vector network analyzer (VNA) that operates in the X-Band. We will place the antenna on a mock CubeSat chassis to replicate the operating environment and connect it to the VNA input port once the VNA has been properly calibrated. We will then setup the VNA to produce a Smith Chart output at several frequencies around 10 GHz. From this graphical representation, we can visualize how well the antenna is matched to the VNA, which has an impedance of 50 ohms.

Voltage Standing Wave Ratio (VSWR)

To measure the VSWR of our antenna, we will use the same VNA that was used to measure the input impedance. We will recalibrate the VNA to ensure that we are getting accurate results and connect the antenna back up to the input port on the VNA. Once the setup is complete, we will use the select the VSWR option on the VNA to measure the VSWR. If the value of the VSWR is close to one, then we will know that our antenna is closely matched to the impedance of the VNA.

S11 Parameter Plot

To produce the S11 Parameter Plot, we will use the same setup that was used to measure the input impedance and VSWR, ensuring that the VNA is re-calibrated before any measurements are taken. Once the antenna is connected to the input port on the VNA, we will run a frequency sweep from around 6 GHz to around 13 GHz and select the S11 Plot option. The resulting plot is a measure of the return loss of the antenna, so if there is a minimum near 10 GHz, then we will know that our antenna operates in the desired frequency band.

Far-Field Radiation Pattern

The radiation pattern will be measured in the anechoic chamber of the RadLab. We will follow a similar procedure to the one used in Lab 2. We will set up our antenna on a mock CubeSat chassis and place it elevated in the chamber. First, we will measure the radiation pattern in the horizontal plane and then we will rotate it 90 degrees to measure the radiation pattern in the vertical plane. Once the antenna is set up with the proper orientation, we will connect it to a signal generator with a center frequency set to 10 GHz with a 100 MHz span. Turn the signal generator on and set the output power to around 10 dBm. Using the Chamber Software on the computer next to the signal generator, select "Far-Field Pattern Measurement" and Initialize the program. Set the antenna to rotate from -135˚to 135˚over 91 positions, a rotator speed of 50, averaging over 2 sample measurements, a 1 second settling time, and a frequency span of 100 MHz. Click measure and wait for the measurements to complete. Once the horizontal pattern has been measured, rotate the antenna and repeat the above procedure. Once the radiation patterns are produced, we can compare the results to those found in the HFSS simulations to verify the design performs as expected.

Future Testing

Before deployment of our CubeSat system, we test several other aspects of our design. Although we would be unable to accomplish all necessary tests during a single semester given the resources available, a few of our proposed tests are explained in the following paragraph. Overall, we need to generally prove that our design will operate in the orbital environment of Ceres. This would involve testing our SAR system at extremely low temperatures and comparing the accuracy of its recordings. Because the temperature in space is much lower than the temperature in Ann Arbor, we need to ensure that our system will operate correctly at these low temperatures. Also, because the surface terrain of Ceres is very soft and consists mostly of water ice [18], we would need to test our SAR system to ensure that it can get accurate readings over this type of surface. We also need to test our design under several conditions to ensure that it will still operate under non-optimal conditions. For example, a major aspect of our antenna is a hinge mechanism that unfolds the antenna after deployment. It is possible that the antenna does not unfold completely while orbiting Ceres so we would need to test the hinge in various orientations to make sure that our design is robust enough to be deployed.

Recommendations for Spaceflight/Future Design Considerations

We recommend several updates to the system for spaceflight. First, the capacitive coupling between waveguide halves needs to be mitigated through some sort of protective covering, and an extremely secure locking mechanism is to be implemented. Lighter materials can also be researched and implemented, or increase the frequency to use a smaller waveguide than WR90. Also, data processing strategies would need to be implemented to process the received data to understand the composition of Ceres more clearly. Lastly, the deployment of the slotted waveguide antenna on the CubeSat would need to be designed and tested.

References

1. http://www.ece.uah.edu/courses/material/EE619-2011/RadarRangeEquation(2)2011.pdf
2. https://www.esa.int/Science_Exploration/Space_Science/Extreme_space/Surviving_extreme_conditions_in_space
3. http://www.geo.uzh.ch/~fpaul/sar_theory.html
4. Wireless Link Design, EECS 430 Coursepack
5. https://solarsystem.nasa.gov/planets/dwarf-planets/ceres/overview/
6. https://www.radartutorial.eu/06.antennas/Fan%20beam%20antenna.en.html
7. http://www.antenna-theory.com/antennas/reflectors/dish3.php
8. https://www.CubeSatshop.com/product/solar-panels/ (EXA Deployable Solar Panels DSA/1A)
9. https://www.endurosat.com/CubeSat-store/all-CubeSat-modules/3u-single-deployable-solar-array
10. http://www.johnstonsarchive.net/astro/radarasteroids.html
11. https://www.sarusersmanual.com/ManualPDF/NOAASARManual_CH01_pg001-024.pdf (PRF equations for data rate bounds, page 13)
12. https://topex.ucsd.edu/rs/sar_summary.pdf (Used for data link design equations)
13. https://ui.adsabs.harvard.edu/abs/2018DPS....5041204B/abstract
14. https://echo.jpl.nasa.gov/asteroids/ostro_1998_encyc_ss.pdf
15. https://www.sciencedirect.com/science/article/abs/pii/0019103579900277
16. https://www.nature.com/articles/s41467-017-00434-6
17. https://www.alternatewars.com/BBOW/Space/Solar_Constant.htm
18. https://solarsystem.nasa.gov/planets/dwarf-planets/ceres/in-depth/
19. https://dsp.stackexchange.com/questions/46930/correct-radar-range-equation-for-snr-at-detection
20. https://www.eorc.jaxa.jp/JERS-1/en/GFMP/SEA-2A/docs/html/imgv3.htm
21. http://www.rfcafe.com/references/electrical/ew-radar-handbook/radar-cross-section.htm
22. https://www.jpl.nasa.gov/cubesat/missions/raincube.php
23. http://www.antenna-theory.com/antennas/aperture/slottedWaveguide.php
24. Chris Heegard and Stephen B. Wicker (1999). *Turbo coding*. Kluwer. p. 3. ISBN 978-0-7923-8378-9.